Copyright Information

BibTeX

```
@INPROCEEDINGS{Fabbri2017distributed,
  author={T. Fabbri and E. Simetti and G. Casalino and L. Pallottino
     and A. Caiti},
  booktitle={OCEANS 2017 - Aberdeen},
  title={Distributed Task-priority Based Control in Area Coverage
     Adaptive Sampling},
  year={2017},
  pages={1-8},
  month={June},
}
```

Distributed Task-priority Based Control in Area Coverage & Adaptive Sampling

T.Fabbri *†‡, E. Simetti*§, G.Casalino*§, L. Pallottino†‡, A. Caiti *†‡

*Interuniversity Center of Integrated Systems for Marine Environment (ISME), Italy
†Dept. of Information Engineering, University of Pisa, Italy
‡ Research Center E. Piaggio, University of Pisa, Italy
§ Dept. Informatics, Bioengineering, Robotics and Systems Engineering, University of Genova, Italy
tommaso.fabbri@for.unipi.it

***Abstract*—The paper presents the first simulative results and algorithmic developments of the task-priority based control applied to a distributed sampling network in an area coverage or adaptive sampling mission scenario. The proposed approach allowing the fulfilment of a chain of tasks with decreasing priority each of which directly related to both operability and safety aspects of the entire mission. The task-priority control is presented both in the centralized and decentralized implementations showing a comparison of performance. Finally simulations of the area coverage mission scenario are provided showing the effectiveness of the proposed approach.**

I. Introduction

In the latest decades, the field of multi-robot system has been object of a widespread research interest resulting in several advantages in terms of safety, time and cost respect to the development of a single autonomous system. In the marine domain, tasks that were considered dangerous, expensive and time consuming when performed by humans can be brilliantly solved by a team of Autonomous Underwater Vehicles (AUVs). High value asset defence, patrolling, exploration, mapping of the seabed represent few of the many practical applications taking advantage of the deployment of a distributed network of mobile sensors.

In this work we face the problem of adaptively governing the motions of a team of AUVs which is employed for performing a distributed sampling mission in order to evaluate an estimate $\hat{\theta}(x)$ of the oceanic field $\theta(x)$ over a predefined Area Of Interest (AOI). In this kind of applications, the selection of the new set of sampling points at each stage represent a crucial task: each new set should be located within no yet explored areas. To avoid useless oversampling the new set should stay at a suitable distance from previous sampled points and presenting at the same time a suitable sparse configuration in order to maintain an *a priori* established measure of quality within preassigned bounds. Furthermore, during the motion towards the selected sampling set, the network nodes have to maintain their connectivity while also maintaining all distances among them above a minimal threshold, for avoiding any risk of collisions within a team or possible obstacles. Finally, the agents have to move to sample points in order to incrementally cover the assigned AOI without the arising of disjoint unexplored zones.

In the recent years, solutions in the field of ocean sampling have been provided in different ways: in [1], [2], [3] mission requirements have been translated in suitable potential functions appropriately combined for the field estimate task or other kind of mission; in [4] the environmental sampling mission has been faced through an adaptive planning approach where the new sampling points are selected via a fuzzy-like algorithm based on field measurements. Other solutions have been provided through path planning as in [5] and more recently, in [6] the authors have proposed a framework following the sampling on-demanding paradigm.

The idea developed in this paper stems from the work [7] defining the complex mission as chain of sub-tasks with decreasing priority, with the objective in mind that the high priority tasks can not be affected by low priority ones. In the distributed systems, this idea has already been extensively addressed (in the land domain) in [8], [9] through the sub-optimal approach defined as Null-Space-based Behaviour (NSB) where the use of a supervisor for the coordination of tasks may lead to undesired discontinuities. In this paper to control the distributed sampling network we propose the Task-Priority based Control (TPC) integrating inequality control objectives [10] able to overcome those limitations, maintaining the structure of a prioritized control.

The paper is organized as follows. Section II describes the task-priority framework applied to the distributed network of AUVs focusing on the chain of tasks involved in the mission. Section III briefly provides a description of the approach followed to realize a decentralized control scheme. Section IV presents the exploration policy developed as final as lower priority task in the framework. Simulations comparing the centralized and decentralized control scheme and a complete area coverage mission are presented in Section V. Finally, Section VI concludes the paper with final considerations and indications about the future work to be developed.

II. The Task-Priority Framework

The task priority based control is a formalism allowing the design of complex control laws able to exploit the kinematic redundancies in robotic systems [10]. Redundant degrees of freedom can be exploited for the fulfilment of a number of

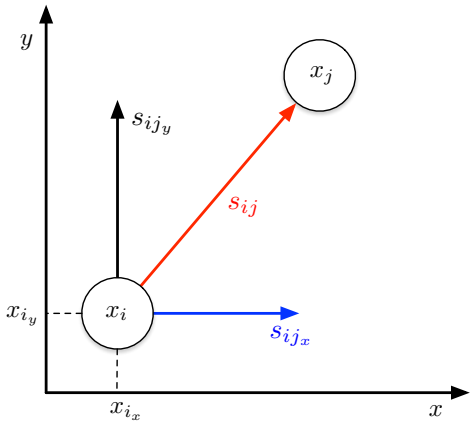

Fig. 1: Distance vector among two nodes composed of two components in the planar scenario.

functional constraints which give dexterity and versatility to the robot in terms of interaction with the environment. The task priority based control enables the execution of the low priority tasks without affecting the execution of the high priority ones. In this paper, the task priority based control is applied to a distributed network of moving agents which can be assimilated to a robotic kinematic chain (even if of a very particular nature).

In this implementation the task priority based control integrates inequality control objectives and task transitions as described in [7], [10]. As mentioned the robotic system considered is a network of moving agents like AUVs. During the motion of the team, the agents are required to maintain their connectivity while also maintaining security distances among them for avoiding the risk of collisions within the team and finally moving towards the specified preferential exploration direction.

A. The Robotic System

The network of moving agents represents the particular kinematic chain involved in this paper. The network topology is described by a graph $\mathcal{G} = (V, E)$ composed by a finite set of *nodes* V (the agents) and a set of *edges* $E \subset V \times V$ connecting the pairs of nodes. The agents set $V = x_1, x_2, \ldots, x_n$ has $N = |V|$ elements, while the edge set $E = e_1, e_2, \ldots, e_m$ has $M = |E|$ elements which may vary along the mission. The graph edges are to be interpreted as a flow information between the agents of the corresponding edge. In this context we consider an undirected graph due to bidirectional communication among the agents. Each agent x_i is described by its planar configuration $\left[x_{i_x}, x_{i_y}\right]^T$ $i = 1, 2 \ldots N$. Each edge $e_j \in E$ $j = 1, 2 \ldots M$ is described by a vector $\boldsymbol{s}_{ij} = \left[s_{ij_x}\ s_{ij_y}\right]^T$ which directly connect i and $j \neq i$ within $\mathcal{G}$. The module σ_{ij} of vector $\boldsymbol{s}_{ij}$ represent the distance between the nodes of the network. The quantities defined above are depicted in Figure 1 for the planar dimensional case. The dynamic evolution of the robotic system analysed in this paper

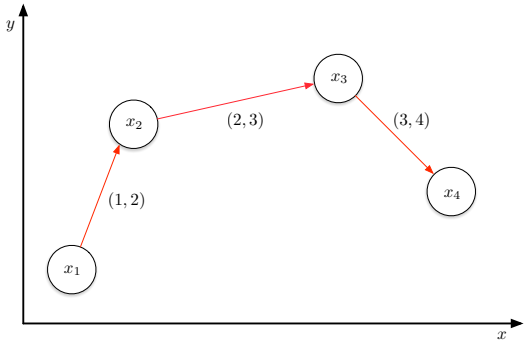

Fig. 2: Example of network composed of 4 nodes connected through 3 edges.

is defined by

$$\dot{\sigma}_{ij} = J_{ij}\dot{X} \tag{1}$$

where J_{ij} maps the velocities of each node $\dot{X} = \mathrm{col}(\dot{x}_i,\ i = 0, 1, \ldots, N)$ (for the planar case $\dot{X} \in \mathbb{R}^{N\times 2}$) into time variation of relative distances among the linked nodes (or time evolution of the length of each edge) . The Equation (1) can be rewritten in a vectorial form as follows in Equation (2):

$$\dot{\sigma}_{ij} = \underbrace{\begin{bmatrix} 0 \ \ldots\ 0 & \overbrace{\frac{\boldsymbol{s}_{ij}^T}{\sigma_{ij}}}^{i^{\text{th}}} & 0 \ \ldots\ 0 & \overbrace{-\frac{\boldsymbol{s}_{ij}^T}{\sigma_{ij}}}^{j^{\text{th}}} & 0 \ \ldots\ 0 \end{bmatrix}}_{J_{ij}} \left.\begin{bmatrix} \dot{x}_1 \\ \vdots \\ \dot{x}_i \\ \vdots \\ \dot{x}_j \\ \vdots \\ \dot{x}_N \end{bmatrix}\right\} \dot{X} \tag{2}$$

The Equation (2) is valid for each edge $(i, j) \in E$ obtaining the following compact representation:

$$\dot{\Sigma} = J\dot{X} \tag{3}$$

where $\dot{\Sigma}$ collects the variation rates of the relative distances σ_{ij} $\forall (i, j) \in E$ and J is the Jacobian of the network of agents system considered. This Jacobian is characterized by high sparsity, and the singularities of the matrix J happen only when two agents are located in the same position. To have a better view of the proposed description of the system, we consider as an example a network of nodes composed of 4 agents connected through 3 edges as depicted in Figure 2. The structure of Equation (3) for this example assumes the following shape:

$$\begin{bmatrix} \dot{\sigma}_{12} \\ \dot{\sigma}_{23} \\ \dot{\sigma}_{34} \end{bmatrix} = \begin{bmatrix} \frac{\boldsymbol{s}_{12}^T}{\sigma_{12}} & -\frac{\boldsymbol{s}_{12}^T}{\sigma_{12}} & 0 & 0 \\ 0 & \frac{\boldsymbol{s}_{23}^T}{\sigma_{23}} & -\frac{\boldsymbol{s}_{23}^T}{\sigma_{23}} & 0 \\ 0 & 0 & \frac{\boldsymbol{s}_{34}^T}{\sigma_{34}} & -\frac{\boldsymbol{s}_{34}^T}{\sigma_{34}} \end{bmatrix} \begin{bmatrix} \dot{x}_1 \\ \dot{x}_2 \\ \dot{x}_3 \\ \dot{x}_4 \end{bmatrix} \tag{4}$$

The evolution of the relative distances among the connected agents of sampling network are required as task variables for the fulfilment of the connection-keeping and collision-avoidance tasks, described in Section II-B and Section II-C.

In order to move the sampling network towards new preferential exploration directions a new task variable has to be defined. As described in detail in Section IV, during each sampling-stage each node of the sampling network identifies a point $\boldsymbol{p}_i$ within the AOI. Starting from such point, the vector $\boldsymbol{s}_{ip_i}$ "linking" each node x_i with the associated point $\boldsymbol{p}_i$ is defined. The module σ_{ip_i} of the vector $\boldsymbol{s}_{ip_i}$ represents the distance between the node and the associated point. The dynamic evolution of the distance σ_{ip_i} is defined as follows

$$\dot{\sigma}_{ip_i} = \frac{\boldsymbol{s}_{ip_i}^T}{\sigma_{ip_i}} \dot{\boldsymbol{x}}_i \tag{5}$$

The Equation (5) can be rewritten in a vectorial form as follows:

$$\dot{\sigma}_{ip_i} = \underbrace{\begin{bmatrix} 0 & \dots & 0 & \overbrace{\frac{\boldsymbol{s}_{ip_i}^T}{\sigma_{ip_i}}}^{i^{\text{th}}} & 0 & \dots & 0 \end{bmatrix}}_{J_{ip}} \begin{bmatrix} \dot{x}_1 \\ \vdots \\ \dot{x}_i \\ \vdots \\ \dot{x}_N \end{bmatrix} \dot{X} \tag{6}$$

Considering a connected graph, the relation defined in Equation (6) for the whole network considering an unique point p associated to each node takes the following compact representation:

$$\dot{\Sigma}_p = J_p \dot{X} \tag{7}$$

where $\dot{\Sigma}_p$ collects all the relative velocities $\dot{\sigma}_{ip}$ $i = 1, 2, \dots, N$, J_p is the new configuration-dependent task Jacobian.

$$\begin{bmatrix} \dot{\sigma}_{1p_1} \\ \dot{\sigma}_{2p_2} \\ \dot{\sigma}_{3p_3} \\ \dot{\sigma}_{4p_4} \end{bmatrix} = \begin{bmatrix} \frac{\boldsymbol{s}_{1p_1}^T}{\sigma_{1p_1}} & 0 & 0 & 0 \\ 0 & \frac{\boldsymbol{s}_{2p_2}^T}{\sigma_{2p_2}} & 0 & 0 \\ 0 & 0 & \frac{\boldsymbol{s}_{3p_3}^T}{\sigma_{3p_3}} & 0 \\ 0 & 0 & 0 & \frac{\boldsymbol{s}_{4p_4}^T}{\sigma_{4p_4}} \end{bmatrix} \begin{bmatrix} \dot{x}_1 \\ \dot{x}_2 \\ \dot{x}_3 \\ \dot{x}_4 \end{bmatrix} \tag{8}$$

B. Task I: Connection keeping

The first objective to be fulfilled is the connectivity-keeping among the agents composing the network. To this end, the following constraint is defined:

$$\sigma_{ij} < d_M \tag{9}$$

where d_M represents the maximum communication range. For each connecting edge is associated a reference rate $\dot{\bar{\sigma}}_{ij}^1$ capable of driving the associated agents towards to the corresponding objective. To satisfy the connection keeping among the agents linked by an edge, the following *feedback reference rate* is defined:

$$\dot{\bar{\sigma}}_{ij}^1 = \gamma_1 (d_1 - \sigma_{ij}) \quad \gamma_1 > 0 \quad d_1 < d_M \tag{10}$$

which represents a feedback law that, whenever directly applied would be capable to drive σ_{ij} towards an arbitrarily chosen value d_1 inside the interval where the inequality is satisfied. Based of the framework developed in [10] the connection-keeping task can be enabled or disabled based on the fulfilment of the Equation (9). More precisely an *active task* is defined as the requirement of tracking at best reference rate $\dot{\bar{\sigma}}_{ij}^1$ in the current operational condition, while an *inactive task* is trivially defined as the absence of any tracking requirement of a reference rate $\dot{\bar{\sigma}}_{ij}^1$. Each feedback reference rate (defined for all edges $(i,j) \in E$) is therefore associated with a *feedback activation function* $\alpha_{ij}^1(\sigma_{ij})$ of sigmoidal type as depicted in Figure 3. At this stage the problem can be faced as the evaluation at each time instant the set S_1 of agents velocities $\dot{X}$ minimizing the following:

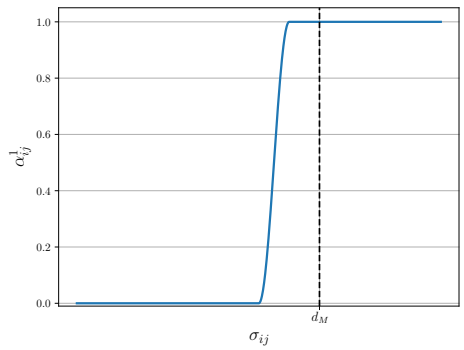

Fig. 3: Feedback activation function for the connection-keeping task.

$$S_1 = \{\dot{X} = \arg\min_{\dot{X}} \sum_{(i,j)\in E} \|\alpha_{ij}^1 (\dot{\bar{\sigma}}_{ij}^1 - J_{ij}\dot{X})\|^2\} \tag{11}$$

Keeping into account the definition of the feedback reference rate $\dot{\bar{\sigma}}_{ij}^1$ and the feedback activation function α_{ij}^1, only the agents not satisfying the Equation (9) are pushed toward any arbitrary point inside communication range, while if the task is inactive (i.e. $\alpha_{ij}^1 = 0$) there is no need to to track the requirement of the reference rate. At this stage, the Equation (11) is re-expressed in a more compact form:

$$S_1 = \{\dot{X} = \arg\min_{\dot{X}} \|A_1 (\dot{\Sigma}_1 - J\dot{X})\|^2\} \tag{12}$$

with:

$$\begin{cases} \dot{\Sigma}_1 = \text{col}(\dot{\bar{\sigma}}_{ij}^1) & \forall (i,j) \in E \\ A_1 = \text{diag}(\alpha_{ij}^1) & \forall (i,j) \in E \end{cases} \tag{13}$$

The Equation (12) represent a modification of a well known problem in robotic kinematic chains of finding the set of all joint rates that realizes a given $\dot{\bar{x}}$ at the best in a least-square sense as reported in Equation (14).

$$S_{\dot{Q}} = \{\dot{Q} = \arg\min_{\dot{q}} \|\dot{\bar{x}} - J\dot{q}\|^2\} \tag{14}$$

As matter of fact, the Equations (13) and (14) differs only for the weight diagonal matrix A_1. Then the solution set S_1 follows in terms of the the manifold defined in Equation (15).

$$S_1 = \{\dot{X} = \dot{X}_1 + N_1 \dot{z}_1\} \quad \begin{cases} F_1 = A_1 J \\ \dot{X}_1 = F_1^{\#}(A_1 \dot{\bar{\Sigma}}_1) \\ N_1 = (I - F_1^{\#} F_1) \end{cases} \tag{15}$$

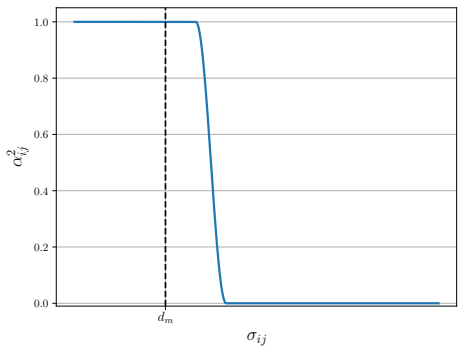

Fig. 4: Feedback activation function for the collision avoidance task.

With $\dot{X}_1$ corresponding to the minimal norm solution to which any vector of the form $N_1\dot{z}_1 \quad \forall \dot{z}_1$ can be added without altering the minimum value of the quadratic form. The operator $\square^{\#}$, appearing on the Equation (15) and in the following of the paper, represents the *regularized pseudo-inverse* proposed in [10] used to the end of managing with continuity the algorithmic singularities that may happen when the value of the various activation functions α^n_{ij} decrease towards zero.

C. Task II: Collision avoidance

The second objective to be fulfilled is the collision avoidance among the agents by forcing all the agents staying each other above a given safety distance d_m. To this end, we consider the following control objective

$$\sigma_{ij} > d_m \quad \forall (i,j) \in E \tag{16}$$

We can proceed in a way strictly similar as before the task of connection-keeping. In first stage we introduce a new feedback reference rate as follows:

$$\dot{\bar{\sigma}}^2_{ij} = \gamma_2(d_2 - \sigma_{ij}) \quad \gamma_2 > 0 \quad d_2 > d_m \tag{17}$$

Together with a feedback activation function $\alpha^2_{ij}(\sigma_{ij})$ of sigmoidal type as show in Figure 4. Then by similarly proceeding as before, we define the following set of solution S_1 conditioned by the fulfilment of the connection-keeping task.

$$S_2 = \{\dot{X} = \arg\min_{\dot{X} \in S_1} \|A_2(\dot{\bar{\Sigma}}_2 - J\dot{X})\|^2\} \tag{18}$$

with:

$$\begin{cases} \dot{\bar{\Sigma}}_2 = \text{col}(\dot{\bar{\sigma}}^2_{ij}) & \forall (i,j) \in E \\ A_2 = \text{diag}(\alpha^2_{ij}) & \forall (i,j) \in E \end{cases} \tag{19}$$

By solving explicitly the minimization problem, the conditioned solution set S_1 as linear manifold follows:

$$S_2 = \{\dot{\chi} = \dot{\chi}_2 + N_2\dot{z}_2\} \quad \begin{cases} F_2 = A_2 J \\ \hat{F}_2 = F_2 N_1 \\ \dot{\chi}_2 = (I - N_1\hat{F}_2^{\#}F_2)\dot{\chi}_1 + N_1\hat{F}_2^{\#}A_2\dot{\bar{\Sigma}}_2 \\ N_2 = N_1(I - \hat{F}_2^{\#}F_2) \end{cases} \tag{20}$$

By construction $S_2 \subseteq S_1$, therefore Equation (20) guarantee the achievement of the priority-one objective (connection-keeping) meanwhile doing their best for also achieving the secondary one (safety distance). The residual additional arbitrary vector $N_2\dot{z}_2$ can be now used for forcing the agents transfers toward the desired locations to perform a exploration, or also a patrolling task.

D. Task III: Move towards the desired exploration direction

The third task to be accomplished by the sampling network is to move towards the desired exploration direction. The preferential direction is identified by a set of points $\boldsymbol{p}_i$ each of which associated to each agent of the network. Thus, by assuming the existence of such collection of points $\boldsymbol{p}_i$ at each sampling stage, it will be now sufficient to consider formerly the set of reference feedback laws defined in Equation (21):

$$\dot{\bar{\sigma}}^3_{ip_i} = -\gamma_3\sigma_{ip_i} \quad \gamma_3 > 0 \quad i = 1 \dots N \tag{21}$$

Then proceeding as before, we get the following definition for the associated set S_3 of solutions:

$$S_3 = \{\dot{X} = \arg\min_{\dot{X} \in S_2} \|(\dot{\bar{\Sigma}}_3 - J_p\dot{X})\|^2\} \tag{22}$$

with:

$$\dot{\bar{\Sigma}}_3 = \text{col}(\dot{\bar{\sigma}}^3_{ip_i}) \quad i = 1, 2, \dots, N \tag{23}$$

Through the same algebra as before now leads to the following updated linear manifold:

$$S_3 = \{\dot{X} = \dot{X}_3 + N_3\dot{z}_3\} \quad \begin{cases} \hat{F}_3 = J_p N_2 \\ \dot{X}_3 = (I - N_2\hat{F}_3^{\#}F_3)\dot{\chi}_2 + N_2\hat{F}_3^{\#}\dot{\bar{\Sigma}}_3 \\ N_3 = N_2(I - \hat{F}_3^{\#}\hat{F}_3) \end{cases} \tag{24}$$

The way the preferential exploration direction is selected is actually independent from the way the Equation (24) is computed, therefore this approach can be applied within different contexts. Furthermore, the arbitrary vector $N_3 z_3$ represents the one to be used to accomplish other tasks e.g. force the nodes to move away from previous sampling points.

III. Decentralized Task-Priority Framework

The Task-priority framework recalled in Section II adopts a centralized point of view, where at central level the new reference velocities for each agent are computed based on the complete knowledge of the state of each node composing the network. In this centralized assumption arises the requirement of an unsustainable full-duplex communication among the nodes composing the network. In our previous work [7] to overcome this limitation we proposed a preliminary *planning phase* then followed by a *open-loop execution phase* with each vehicle reacting independently from the others in the case of local marine current which may drive the node far from its own pre-planned trajectory or in worst cases towards obstacles or other nodes.

An alternative solution (if any) would be that of trying to exploit the sparsity exhibited by the various matrices involved

in the motion control part. Unfortunately enough, however, such sparsity does not allow a direct downgrading toward a decentralized solution. The demonstration of such statement is out of the scope of this paper and will be provided along future works.

The solution provided by this work consists on running the task-priority framework locally on each node based on the information available from its set of neighbours. In other words, the task-priority is run on each of the N nodes composing the network, each of which having a partial knowledge of the entire network. Considering the example illustrated in Figure 2, the task-priority is run on the 4 nodes, where the node x_1 sees the network composed by itself and its neighbour x_2; x_2 sees a network composed of two edges linking with x_1 and x_3 and so on for the other agents x_3 and x_4. Simulations provided Section V proves the effectiveness of the solution proposed in different scenarios.

IV. Exploration Methodology

The lowest-priority task described in Section II-D, defining the control method to shift the sampling network towards the preferential exploration direction, requires as input a set of points $\boldsymbol{p}_i, i = 1, \ldots, N$ within the AOI to which each agent will proceed. In a context of area-coverage or environmental adaptive sampling the selection of such points must belong to areas not yet explored or characterized by high uncertainty requiring therefore a more accurate sampling. Considering an environmental sampling scenario, each sampling point is characterized by an associated circle centred on the corresponding sample coordinates in which the error field is below a predefined precision threshold. A method for the selection of the set of points $\boldsymbol{p}_i$ associated to each agent is described in our previous work [7]: the board of each circle on which each agent is centred (at the end of each sampling stage) can be characterized by one more arcs that can be intended as a "door open" towards not yet explored areas. Therefore, reporting the formulation provided in [7], the criteria to be adopted for the selection of such doors for each agent consists on selecting among all the perimetral points $\boldsymbol{x}_L \in L$ of the AOI such that the vectors $(\boldsymbol{x}_L - \boldsymbol{x}_i) \quad i = 1, \ldots, N$ do not intersect any of the circles associated to the all previous sampling points. Then, from the subset of the perimeter point s$\hat{L}$, $\boldsymbol{p}_t \in \hat{L}$ is the point characterized by the maximum distance from the sampling network as stated in Equation (25) as follows:

$$\boldsymbol{p}_t = \arg\max_{\boldsymbol{p} \in \hat{L}} \left[\min_{i=1,\ldots,N} ||\boldsymbol{p} - \boldsymbol{x}_i|| \right] \tag{25}$$

meaning that we must find the point of the perimeter L characterized by the maximum distance from the sampling network and from which the departing rays can light each each agent x_i without intersecting any of the previous sampling circles. An example of the proposed exploration policy is depicted in Figure 5: the cloud of the previous sampling points (blue dashed circles) makes the set $\hat{L}$ includes the north perimetral points (in red); $\boldsymbol{p}_t$ is selected through the Equation (25) defining therefore the preferential exploration direction for the whole sampling network. During the exploration mission the sampling network can reach a state in which the set of points $\hat{L} = \emptyset$ e.g. the agents have reached a configuration close to the perimeter with many of the previous sampling points closing the way out from the current configuration. In such situation the use of the proposed exploration policy has to be stopped (Equation (25)) and switch to a forced block transfer of the network towards zones that will allow to restart the designed exploration policy. The forced block transfer can be translated into an alternative method for selecting the point $\boldsymbol{p}_t$. This design choice allows to maintain unchanged the chain of tasks and provide only a new input to the lower-priority task. Defined as S_p the set of all previous sampling locations reached by the agents along the mission, the new point $\boldsymbol{p}_f$ is the location in the AOI whose distance from any other measurement point is the largest as defined in Equation (26).

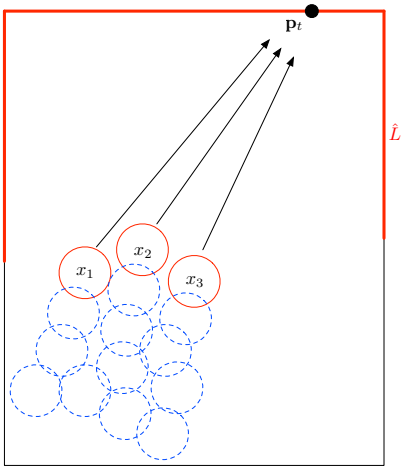

Fig. 5: Example of the proposed methodology for the selection of the preferential exploration direction defined by the perimetral point $\boldsymbol{p}_t$ (selected from the subset of the perimetral points $\hat{L}$ depicted in red).

$$\boldsymbol{p}_f = \arg\max_{\boldsymbol{p} \in \text{AOI}} \left[\min_{\boldsymbol{x} \in S_p} ||\boldsymbol{p} - \boldsymbol{x}|| \right] \tag{26}$$

The new preferential exploration direction could force the sampling network toward areas located beyond already sampled ones requiring the crossing of them without collecting data, for then restarting the policy previously defined in Equation (25) Figure 6 presents an example of the case in which the set of perimetral points $\hat{L}$ is equal to the empty set: in such situation the new preferential direction selected through the Equation (26) drives the sampling network towards areas as far away as possible from the previous sampling points (depicted in blue dashed circles). During the motion may happen that the sampling network crosses already sampled areas (without collecting data on them). Based on the evaluated point $\boldsymbol{p}_t$ (or $\boldsymbol{p}_f$) identifying the preferential exploration direction, each agent of the sampling network is now able to identify its own next sampling point $\boldsymbol{p}_i$. This corresponds to the intersection between the circle associated to the current sampling point

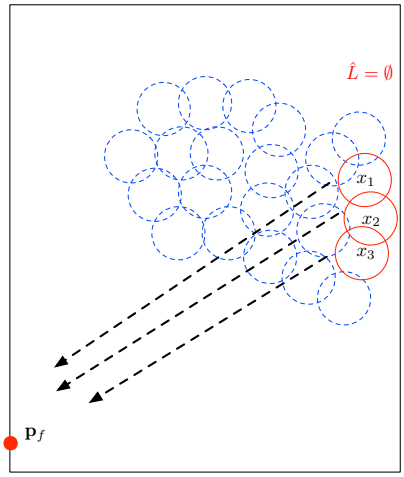

Fig. 6: Example of the proposed methodology for the selection of the preferential exploration direction defined by the perimetral point $\boldsymbol{p}_f$ in the case the $\hat{L} = \emptyset$.

(reached by the agent during the last sampling stage) and the vector linking the agent position with the point $\boldsymbol{p}_t$ (or $\boldsymbol{p}_f$) identifying the preferential exploration direction, as described in [7].

V. Simulative Results

The algorithm testing in simulative scenarios is now reported. In this paper we do not focus on the reconstruction of an environmental field but on the performance analysis of the algorithm in terms of fulfilment of the chain of tasks defined. To make easier the evaluation of the algorithm performance, we consider that all the agents moves at constant depth when transit from one sampling point to another, and the data acquisition happens only when the agents have reached the new sampling point. The sampling agents are able to reach the maximum speed of 2.5 m/s and each vehicle is equipped with acoustic modem allowing the communication within the network if the distance between two agents is less than $d_M = 100$ m. In these simulations, no external disturbances are present.

Figure 10 presents a comparison of the trajectories followed by each agent to reach a desired spatial configuration defined through a set of sampling point p_i $i = 1, \ldots, N$ each of which associated to a sampling agent; the distances among all agents composing the sampling network and the velocity of each agent, both in the centralized and decentralized task-priority control. Such point p_i are supposed to be the results of the intersection between the sampling circles and the preferential exploration direction defined in the previous section. In Figures 10a and 10d the circles with dashed line-style represent the limit of communication range $d_M = 100$ m. Even if the assigned sampling points associated to each agent (the black square markers in Figure 10a and Figure 10d) are located at a distance greater than the maximum communication range d_M, the agents are able to reach a stable configuration with the agents located on the frontier of the communication range as illustrated with the dashed circles in Figures 10a and 10d. Furthermore, in both the centralized and the decentralized task-priority framework the agents moving towards the preassigned sampling points respect the safety distance $d_m = 40$ m. As specified in Section II, the task-priority control always fulfil the highest-priority tasks (connection-keeping and collision avoidance); on the other hand, the lower priority tasks are executed only in the subspace where they do not conflict with the ones at higher priority, as in this example where reaching the specified spatial configuration represents the lower priority task. For this reason, considering the particular scenario of Figure 10, the frontier of the communication range (depicted through dashed dashed circles) of each agent represent the best trade off among all the possible solutions. The simulations shown in Figure 8 demonstrate the fulfilment of collision-avoidance task in both the centralized and decentralized task-priority control when the required spatial configuration is composed of sampling points located at a distance lower than the safety distance $d_m = 40$ m (shown through the dashed circles). Even in the decentralized configuration, where the task-priority control is executed locally on each agent based on the information gathered from the set of neighbours, the agents are able to fulfil the chain of tasks defined.

As shown in these simulations, the control strategy proposed is able to fulfil the chain of tasks defined. In the previous simulations we have considered a set of sampling points $\boldsymbol{p}_i$ $i = 1, \ldots, N$ each of which associated to each agent to prove the fulfilment of the chain of tasks. More precisely, the centralized and decentralized approaches do not present too much differences in the provided simulations. As shown in Figure 10b only the edges of the spanning-tree (composed by the edges [(1,3),(2,4),(3,4)]) at the end of the simulation) are kept below the communication range d_M; instead, in the decentralized control, depicted in Figure 10e, when a link between two nodes is created, the distance between the two nodes involved is kept below the communication range, because no information about the spanning tree is available locally in each agent. As a consequence the resulting network will provide redundant edges in the decentralized approach and a different stable configuration.

By now, focusing on the area coverage or environmental sampling mission scenario, to make easier the evaluation of the proposed exploration methodology we consider a constant sampling radius along the mission and the availability of a designed centre of the network able to compute the preferential exploration direction based on the data collected by the sampling network.

Figure 9 shows a sequence of snapshots at different time-stamp of the trajectories followed by a sampling network composed of three agents during the exploration over a circular area of 250 m of radius. The perimetral markers indicates the preferential exploration directions: black when the point $\boldsymbol{p}_t$ is selected through Equation (25); red when the set $\hat{L} = \emptyset$ and the Equation (26) is used. Furthermore, the solid line style represents the intervals in which the sampling network travels towards the black markers and the dashed line style

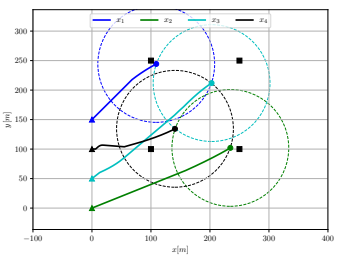

(a) Trajectories of the sampling agents in the centralized task-priority framework.

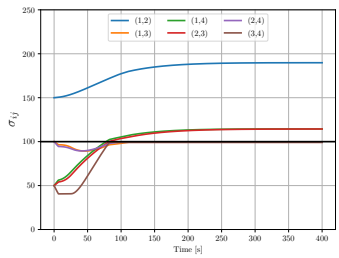

(b) Distance among the sampling agents in the centralized task-priority framework.

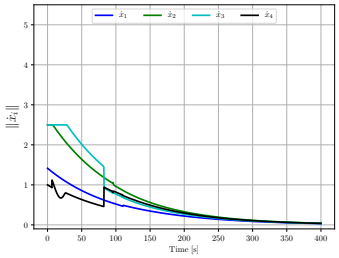

(c) Velocity of the sampling agents in the centralized task-priority framework.

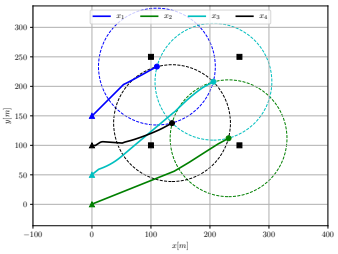

(d) Trajectories of the sampling agents in the decentralized task-priority framework.

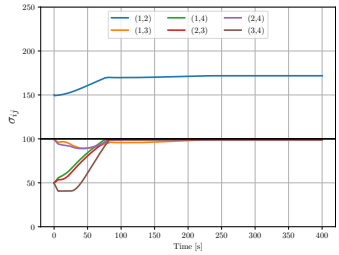

(e) Distance among the sampling agents in the decentralized task-priority framework.

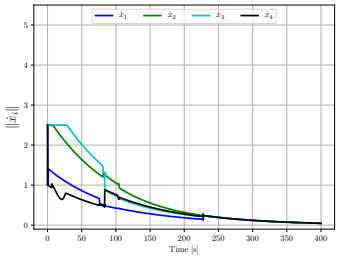

(f) Velocity of the sampling agents in the decentralized task-priority framework.

Fig. 7: Simulations of the centralized (Figures 10a to 10c) and decentralized (Figures 10d to 10f) task-priority control where the sampling network is required to reach a predefined spatial configuration shown through black square markers. Along the simulation the agents are able to maintain the communication range ($d_M = 100$ m, depicted through a dashed circle around each agent) and the safety-distance above the safety limit $d_m = 40$ m.

represents the intervals in which the network travels towards red markers. Finally, the triangle and circle markers represent the starting and end positions respectively for the considered snapshot. As can be seen from the series of mission snapshots, the sampling network moves through the selected "corridor" towards the estimated point $\boldsymbol{p}_t$ until it reaches a state where the set $\hat{L} = \emptyset$ as depicted in Figure 9a: the sampling network has reached a configuration close to the perimeter (south band of the area), and the exploration policy depicted in Figure 5 has to be stopped. At this stage, the forced block transfer is executed, moving the sampling network towards the red marker on the north side of the area identified through the Equation (26). During the shift towards the new preferential direction of exploration, the sampling network is forced towards areas located beyond already sampled ones requiring the crossing of them without collecting data; this behaviour is depicted with dashed line style in Figure 9. During the whole mission the network of agents is able to cover almost the whole area, leaving some spots not covered. Analysis of the mission time required for covering the whole area represent topic of future works.

VI. Conclusions

This paper has presented the first simulative results of the task-priority based control applied to distributed sampling network involved in an area coverage or adaptive sampling mission scenario. Simulations demonstrate that the definition of a chain of tasks and their linked priorities allow the fulfilment of the mission guaranteeing operability and safety aspects of the entire sampling system, both from a centralized and decentralized point of view. Future works will be focus on a deeper formalization of the decentralized approach which will be validated by relevant simulations activities modelling constraints characterizing the underwater environment (e.g. communication frequency ...).

Acknowledgment

This work has been executed within the project RIMA: Mediterranean Integrated Forecast Network for the Management of the Marine Environment; under contract MIUR No DM62617; coordinated by DLTM (District on Marine Technologies - La Spezia, Italy).

References

[1] A. Munafò, E. Simetti, A. Turetta, A. Caiti, and G. Casalino, "Autonomous underwater vehicle teams for adaptive ocean sampling: a data-driven approach," *Ocean Dynamics*, vol. 61, no. 11, pp. 1981–1994, 2011.

[2] F. Fabiani, D. Fenucci, T. Fabbri, and A. Caiti, "A passivity-based framework for coordinated distributed control of auv teams: Guaranteeing stability in presence of range communication constraints," in *OCEANS 2016 MTS/IEEE Monterey*. IEEE, 2016, pp. 1–5.

[3] ——, "A distributed, passivity-based control of autonomous mobile sensors in an underwater acoustic network," *IFAC-PapersOnLine*, vol. 49, no. 23, pp. 367–372, 2016.

[4] A. Caiti, A. Munafò, and R. Viviani, "Adaptive on-line planning of environmental sampling missions with a team of cooperating autonomous underwater vehicles," *International Journal of Control*, vol. 80, no. 7, pp. 1151–1168, 2007.

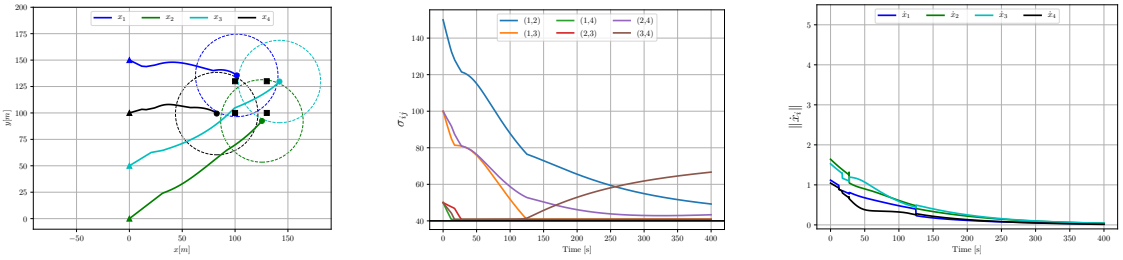

(a) Trajectories of the sampling agents in the centralized task-priority framework.

(b) Distance among the sampling agents in the decentralized task-priority framework.

(c) Velocity of the sampling agents in the decentralized task-priority framework.

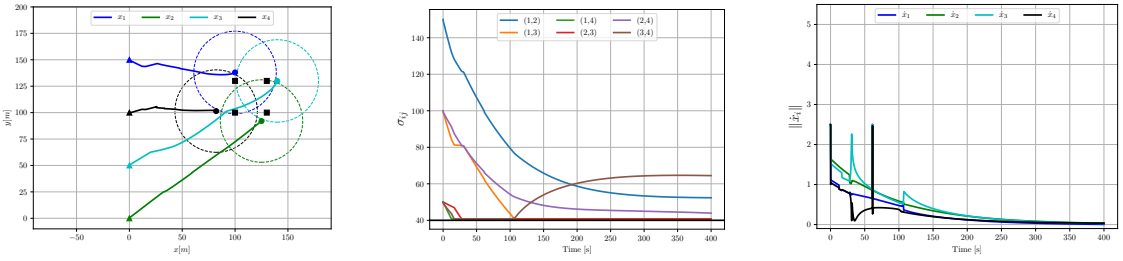

(d) Trajectories of the sampling agents in the decentralized task-priority framework.

(e) Distance among the sampling agents in the decentralized task-priority framework.

(f) Velocity of the sampling agents in the decentralized task-priority framework.

Fig. 8: Simulations of the centralized (Figures 8a to 8c) and decentralized (Figures 8d to 8f) task-priority control where the sampling network is required to reach a predefined spatial configuration shown through black square markers. Along the simulation the agents are able to maintain the distance among them above the safety limit ($d_m = 40$ m, depicted through a dashed circle around each agent) even if the desired sampling point are placed at distance less than the safety limit.

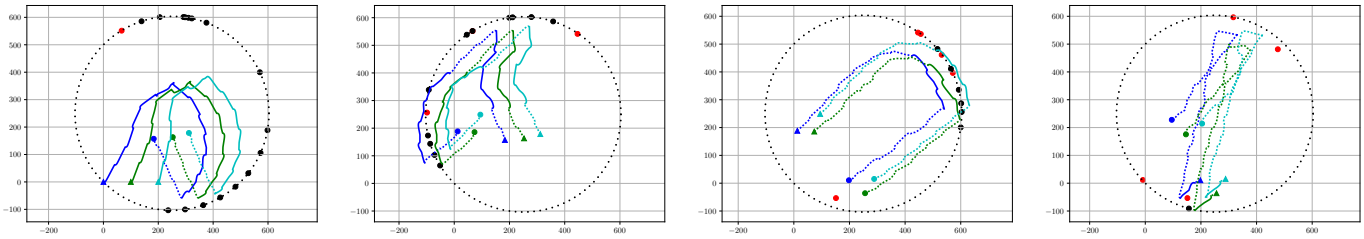

(a) (b) (c) (d)

Fig. 9: Simulation of the exploration task over a circular area with radius of 250 meters depicted through different snapshots at different time-stamp. The black perimetral markers indicate the points p_t selected through the Equation (25), the red markers indicates the points p_f selected through the Equation (26). The dashed line style represents the intervals in which the sampling network travels towards the red markers, the solid line style represents the intervals in which the network travels towards black markers.

[5] A. Alvarez, A. Caiti, and R. Onken, "Evolutionary path planning for autonomous underwater vehicles in a variable ocean," *IEEE Journal of Oceanic Engineering*, vol. 29, no. 2, pp. 418–429, April 2004.

[6] G. Ferri, M. Cococcioni, and A. Alvarez, "Mission planning and decision support for underwater glider networks: A sampling on-demand approach," *Sensors*, vol. 16, 2016. [Online]. Available: http://www.mdpi.com/1424-8220/16/1/28

[7] A. Caiti, E. Simetti, and G. Casalino, "A task-priority based control approach to distributed data-driven ocean sampling," in *OCEANS 2016 - MTS/IEEE Monterey*, Sept 2016.

[8] G. Antonelli, F. Arrichiello, and S. Chiaverini, "The null-space-based behavioral control for autonomous robotic systems," *Intelligent Service Robotics*, vol. 1, no. 1, pp. 27–39, 2008. [Online]. Available: http://dx.doi.org/10.1007/s11370-007-0002-3

[9] A. Marino, L. E. Parker, G. Antonelli, and F. Caccavale, "A decentralized architecture for multi-robot systems based on the null-space-behavioral control with application to multi-robot border patrolling," *Journal of Intelligent & Robotic Systems*, vol. 71, no. 3, pp. 423–444, 2013. [Online]. Available: http://dx.doi.org/10.1007/s10846-012-9783-5

[10] E. Simetti and G. Casalino, "A novel practical technique to integrate inequality control objectives and task transitions in priority based control," *Journal of Intelligent & Robotic Systems*, vol. 84, no. 1, pp. 877–902, 2016.